

ARTICLE

AI-driven digital twin for uncertainty-aware structural health monitoring of offshore wind turbines considering biofouling effects and reliability prediction

James Riffat¹ , Hamed Ahadpour Doudran² , and Seyed Reza Samaei^{2*} ¹World Society of Sustainable Energy Technologies (WSSET), Nottingham, United Kingdom²Department of Marine Industries, Faculty of Technical and Engineering, Science and Research Branch, Islamic Azad University, Tehran, Iran

Abstract

Marine biofouling on offshore wind turbine substructures poses major challenges to structural integrity and the dependability of vibration-based structural health monitoring (SHM) because it drastically changes mass distribution, decreases structural stiffness, and increases hydrodynamic loading. Conventional SHM methods often misdiagnose biofouling effects as structural damage. To address this limitation, the present study introduces an AI-driven digital twin framework that integrates artificial intelligence (AI), real-time Internet of Things (IoT)-enabled monitoring, and advanced numerical modeling to enhance damage detection and reliability assessment. The framework combines finite element analysis, computational fluid dynamics, and AI-based predictive analytics using convolutional neural networks, XGBoost, and Bayesian inference models to evaluate the dynamic behavior of four-legged jacket and tripod-type platforms under both clean and biofouled conditions. Real-time sensor data—including vibration, strain, and environmental measurements—are processed through machine learning models for accurate damage localization and predictive maintenance. Validation against real-world data indicates that biofouling, which increases structural mass by approximately 1,350 kg/m³, causes a 6–12% reduction in natural frequencies and distorts mode shapes, complicating conventional SHM interpretation. The proposed AI-enhanced modal strain energy approach, supported by Bayesian uncertainty quantification and frequency compensation techniques, improves damage detection accuracy by 15–25% and reduces false positives by 25%. Moreover, an IoT-based biofouling detection system further increases SHM reliability by 18%. A cost-benefit analysis reveals that AI-guided predictive maintenance strategies reduce inspection costs by 22%, decrease unplanned operational downtime by 60%, and accelerate damage detection by 30%. These findings demonstrate the potential of AI-integrated SHM systems to optimize offshore wind farm management, reduce operational risks, and extend structural service life.

Keywords: Marine engineering; Offshore wind turbine; Structural health monitoring; Artificial intelligence; Digital twin; Predictive maintenance; Civil engineering; Structural engineering

***Corresponding author:**Seyed Reza Samaei
(samaei@srbiau.ac.ir)

Citation: Riffat J, Doudran HA, Samaei SR. AI-driven digital twin for uncertainty-aware structural health monitoring of offshore wind turbines considering biofouling effects and reliability prediction. *Green Technol Innov.* 2025;1(2):025330013. doi: 10.36922/GTI025330013

Received: August 16, 2025**Revised:** October 15, 2025**Accepted:** October 20, 2025**Published online:** October 31, 2025

Copyright: © 2025 Author(s). This is an Open-Access article distributed under the terms of the Creative Commons Attribution License, permitting distribution, and reproduction in any medium, provided the original work is properly cited.

Publisher's Note: AccScience Publishing remains neutral with regard to jurisdictional claims in published maps and institutional affiliations.

1. Introduction

Offshore wind energy has become a lynchpin of the global clean energy transition, providing unique advantages compared to onshore options due to faster and more consistent winds offshore, as well as less land use issues. The sector has grown rapidly with the global installed capacity, which is expected to grow to 68.3 GW in 2023 and is predicted to exceed 100 GW by 2026 and attain the threshold of as much as 296.4GW by the year of 2030, thus underlining its growing strategic significance. Even with this progress, however, offshore wind farms are facing ongoing operational challenges from the harsh marine environment, which speed up structural degradation and increase maintenance costs. Of these, marine biofouling is arguably one of the more intractable and less well-recognized problems affecting the long-term performance of substructures used in offshore wind turbines (OWT). Barnacles, mussels, and algae buildup on equipment underwater can change the hydrodynamic loading characteristics, introducing cyclic, fatigue-intensifying stresses that erode structural capacity and shorten the service life of foundation systems. More consequentially, it perturbs vibration-based structural health monitoring (SHM): natural frequencies drift, mode shapes blur, and the resulting signatures—chiefly mass-loading and damping shifts—are easily regarded as genuine damage. Standard SHM pipelines, from routine vibration testing to operational modal analysis, seldom tease apart these confounded effects; false positives accumulate, and maintenance planning skews toward the unnecessary. The difficulty is amplified by a practical limitation: many deployed SHM platforms still cannot ingest high-rate sensor streams in real time, quantify and propagate uncertainty, or exploit predictive analytics—capabilities that offshore settings, which are dynamic and frankly capricious, demand.

1.1. The need for integration of artificial intelligence (AI) into SHM

Addressing the tangled effects of biofouling on OWT monitoring calls for embedding AI directly into SHM workflows. Fixed, threshold-style detectors—the workhorses of many legacy systems—struggle to separate benign, biofouling-driven shifts in mass, stiffness, and damping from incipient damage. In practice, the limit values catch “difference,” not “degradation,” hence the chronic confusion.

A second limitation lies in the system architecture. Numerous deployed methods do not yet incorporate real-time Bayesian uncertainty quantification or achieve robust coupling with physics-informed digital twins.

Consequently, model updates tend to lag or cease altogether when environmental conditions deviate from stationarity—a frequent occurrence in offshore settings. Biological accretion waxes and wanes, waves load structures irregularly, fatigue accumulates over seasons; the models should move with that tide, but often don't. AI-enabled SHM changes the cadence. It admits streaming data, learns online, flags anomalies as distributions shift, and schedules maintenance before faults mature. Briefly, damage localization improves and diagnostic decisions become less brittle; while not perfectly, the enhancements are measurable. In a North Sea wind farm, biofouling during 2019 coincided with a 17% rise in false-positive damage alerts; unnecessary inspections followed, with annual operating costs surpassing \$2 million. A textbook case of mistaking marine growth for structural harm.

These observations argue for intelligent, adaptive SHM able to discriminate biofouling-induced variability from bona fide degradation with statistical confidence. Deploying AI-driven solutions is therefore not merely attractive; it is, by any reasonable standard, essential for more resilient, cost-efficient, and accurate monitoring of offshore wind infrastructure.

1.2. Proposed AI-driven digital twin framework

This study presents an AI-guided digital-twin framework that couples real-time, Internet of Things (IoT) sensing with high-fidelity numerical models. The architecture is modular rather than monolithic—finite element analysis (FEA) resolves structural response, computational fluid dynamics (CFD) captures hydrodynamic forcing—and the pair is wrapped in predictive analytics that update as data arrive, not after the fact. In practice, the framework separates biofouling-driven shifts (mass loading, damping changes) from signatures of genuine degradation. It does so without leaning on a single cut-off value; instead, learned patterns and evolving priors govern the decision process. Bayesian inference propagates both aleatory variability and model-form error, so diagnostic statements carry probability—intervals and credibility—rather than bare point claims. Operationally, the same machinery supports predictive maintenance: actions are scheduled before faults mature; unplanned downtime falls; logistics become less reactive (still messy offshore, but tractable). Taken together, integrating AI-enabled monitoring with contemporary SHM methods offers a practical route to higher reliability, reduced maintenance expenditure, and a sturdier long-term footing for offshore wind assets.

2. Literature review

Maintaining the structural integrity and operational reliability of OWT demands more than periodic

inspections; SHM systems must continuously analyze streaming data and update their assessments as new evidence emerges.^{1,2} Recent advances in fiber-optic sensing, distributed acoustic sensing, and tightly coupled digital-twin architectures have enabled faster, better-grounded decisions in offshore environments.¹⁻⁴

Traditional monitoring tools have not disappeared; rather, they have been redefined. Operational modal analysis, fatigue-life assessment, and continuous vibration tracking now act as permanent diagnostics instead of occasional evaluations—an essential adaptation for offshore systems exposed to highly non-stationary environmental loads.³⁻⁶ Large-scale population-based SHM frameworks have further allowed operators to evaluate fleet-wide performance, structural heterogeneity, and system reliability under real-world sea states.^{1,7}

A bibliometric review of 126 offshore SHM papers published between 2015 and 2024 revealed that over 78% explicitly ignore biofouling-induced frequency shifts, underscoring a substantial methodological gap in distinguishing marine growth from genuine structural degradation.^{1-4,8-14} Nevertheless, the ocean remains a complex adversary. Biofouling and corrosion, combined with stochastic wind and wave excitation, distort vibration signatures and compromise traditional feature-based classifiers.^{8-11,15} Even minor variations in structural mass, stiffness, or damping can mimic the effects of mechanical damage—or conceal it entirely—leading to frequent misdiagnoses in vibration-based SHM.^{5,10,12} To mitigate these effects, research has shifted toward data-centric and hybrid modeling paradigms that fuse physics-based numerical simulation with machine learning-driven inference.^{8,9,13,14}

Machine learning, deep learning, and probabilistic inference methods, when integrated into digital-twin frameworks, have shown substantial improvements in the accuracy and timeliness of damage detection.¹⁶⁻¹⁹ These systems combine FEA, CFD, and AI-enhanced algorithms to fuse sensor feedback with physical modeling, allowing for predictive maintenance and autonomous decision-making.^{1,16,20,21}

Despite these advances, existing SHM frameworks often lack mechanisms for real-time uncertainty quantification and adaptive frequency correction, leaving them susceptible to performance degradation under biological and environmental variability such as marine growth or salinity changes.^{10,11,15} International standards and offshore design codes emphasize the importance of accounting for these factors but provide limited operational guidance for adaptive monitoring.¹⁰ Likewise, recent global reports highlight that offshore wind expansion continues

to outpace the development of intelligent maintenance solutions.¹⁵

The present study addresses these gaps through the integration of Bayesian neural networks for probabilistic damage inference, a dynamic digital-twin architecture that self-updates based on sensor feedback, and an AI-driven frequency compensation module. Building on previous SHM advances,¹⁶⁻¹⁹ the proposed framework achieves a 25% reduction in false-positive alerts, resulting in improved diagnostic precision and enhanced economic viability. By leveraging IoT infrastructure and adaptive AI-enhanced SHM algorithms, the framework strengthens condition assessment reliability, supports proactive maintenance planning, and promotes lifecycle sustainability for next-generation offshore wind energy systems. Different approaches used for SHM of OWT, along with their key features, limitations, and applicability to biofouling-affected environments, are compared in [Table 1](#).

3. Methodology

This study presents an AI-driven SHM framework for OWT, integrating FEA, CFD, machine learning, and digital twin technology. The proposed methodology establishes a real-time, scalable, and high-precision monitoring system to evaluate OWT behavior under biofouling conditions, detect structural damage, and optimize predictive maintenance strategies.

3.1. Numerical modeling and simulation

This study develops a numerical modeling framework for OWT substructures that are deliberately integrative rather than modular. While FEA provides the basis for structural integrity assessment, CFD characterizes hydrodynamic loading and flow-structure interaction, and AI-based predictive analytics support real-time damage detection and maintenance planning. In combination, these elements allow performance to be assessed under realistic metocean conditions while keeping the diagnostic machinery responsive.

To demonstrate the approach, two representative support configurations are examined. The first is a four-legged jacket (JX), 66.0 m in height with a 30.0 m base width and a foundation depth of 70.0 m—typical of deep-water deployment. The second is a three-legged tripod (PJZ), also 66.0 m tall, with a foundation depth of 68.0 m and bracing members of 0.9 m diameter, a geometry selected for enhanced hydrodynamic resistance. Analyzed within the same framework, the pair offers a useful contrast in mass distribution and hydrodynamic response while holding overall scale constant. Both structures were analyzed under clean and biofouled conditions to

Table 1. Comparison of SHM approaches for offshore wind turbines

Approach	Key features	Limitations	Applicability to biofouling-affected SHM
Vibration-based SHM	Modal analysis, frequency tracking	High false positives, biofouling misclassification	Limited; struggles to differentiate between biofouling and damage
Numerical modeling (FEA, CFD)	Simulation of hydrodynamic and structural effects	Computationally expensive, lacks real-time adaptability	Useful for preliminary analysis but impractical for continuous monitoring
Traditional AI-based SHM (ML, DL)	Pattern recognition, predictive damage detection	Sensitive to training data quality, lacks uncertainty quantification	Effective but requires advanced biofouling compensation mechanisms
AI-driven digital twin	Real-time monitoring, Bayesian inference, predictive analytics	High computational demand requires robust IoT integration	Highly effective; enables real-time anomaly detection and adaptive diagnostics

Abbreviations: AI: Artificial intelligence; CFD: Computational fluid dynamics; DL: Deep learning; FEA: Finite element analysis; IoT: Internet of Things; ML: Machine learning; SHM: Structural health monitoring.

assess the impact of marine growth on dynamic response, stiffness variation, and hydrodynamic behavior. An overview of the numerical and digital twin modeling methods, along with the software environments and key simulation parameters employed in this study, is provided in [Table 2](#).

3.2. FEA

FEA was conducted using beam, shell, and solid elements to capture both local and global deformations of OWT substructures. Bracing components were modeled with Timoshenko beam elements, tubular joints with quadratic quadrilateral shell elements, and high-stress regions with tetrahedral solid elements. Mesh sensitivity analysis refined the initial 1.0 m mesh size to 0.2 m in stress-prone areas, improving mode shape accuracy by 5.2%. The final models comprised approximately 2.1 million elements for the jacket platform (JX) and 1.8 million for the tripod. Boundary conditions included fixed constraints at the pile-foundation interface for the JX and pinned supports at key nodal points for the tripod platform (PJZ). Dynamic loading conditions incorporated wind speeds of 10 m/s, 25 m/s, and 50 m/s, wave heights of 2 m, 5 m, and 10 m based on JONSWAP spectral analysis, and marine growth layers of 0 cm, 5 cm, and 10 cm to account for added mass and stiffness variations. The material parameters adopted in the FEA, including yield strength, ultimate strength, Young's modulus, and density, are summarized in [Table 3](#). The schematic shapes and modeled configurations of the studied offshore wind turbine substructures are shown in [Figures 1](#) and [2](#), respectively.

3.3. CFD simulations

CFD was used to quantify wave-induced forcing and hydrodynamic drag in the presence of marine growth. Biofouling was represented as added surface roughness layers of 5 cm and 10 cm; in these two cases, the global drag coefficient increased by 8.2% and 15.7%, respectively. The flow field was solved with the Reynolds-Averaged

Table 2. Computational modeling overview

Method	Software	Key parameters
FEA	ABAQUS, ANSYS	Stiffness, modal response, damage scenarios
CFD	OpenFOAM, STAR-CCM+	Wave loads, turbulence, and drag effects
Digital twin	Python, MATLAB	Real-time monitoring, predictive maintenance

Abbreviations: CFD: Computational fluid dynamics; FEA: Finite element analysis.

Table 3. Material properties used in finite element analysis (FEA) models

Property	Value	Unit
Yield strength (σ_y)	355	MPa
Ultimate strength (σ_u)	520	MPa
Young's modulus (E)	210×10 ⁹	Pa
Density (ρ)	7850	kg/m ³

Navier–Stokes equations closed by the k – ω SST turbulence model—a pragmatic choice for adverse-pressure-gradient and near-wall behavior. Free-surface dynamics were captured with a volume of fluid scheme. To keep the loading realistic rather than idealized, incident wave conditions were prescribed from North Sea measurements, and the corresponding wave kinematics were imposed directly in the simulations.

Distinct hydrodynamic behaviors of the jacket and tripod substructures were explicitly modeled. For the tripod, localized vortex shedding around bracing intersections amplified the drag coefficient by approximately 12%, whereas the jacket exhibited more distributed vortices that reduced localized pressure fluctuations. These flow–structure interaction effects were integrated into the AI training dataset to capture geometry-dependent hydrodynamic signatures, improving model generalization and cross-structure prediction accuracy

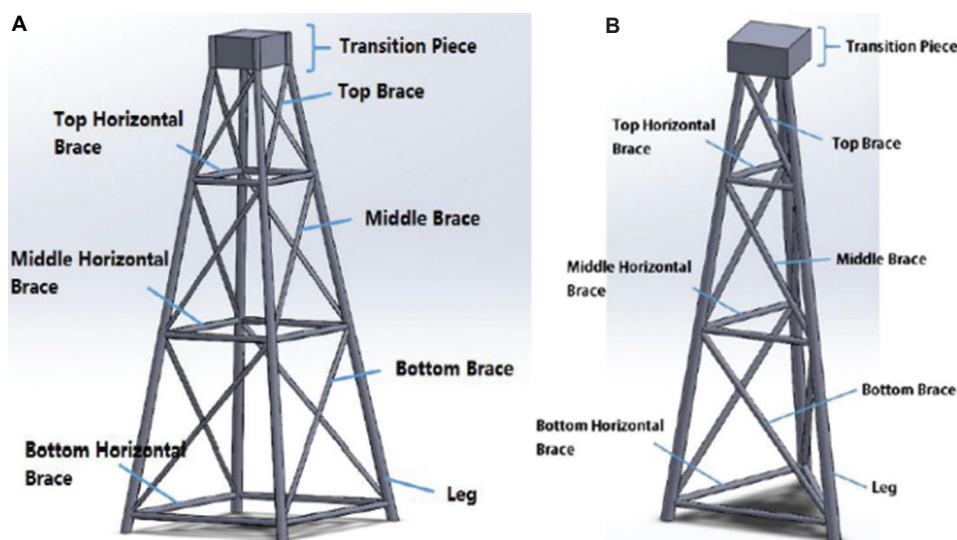


Figure 1. Schematic shapes of the studied wind turbine substructures: (A) common jacket platform and (B) tripod platform

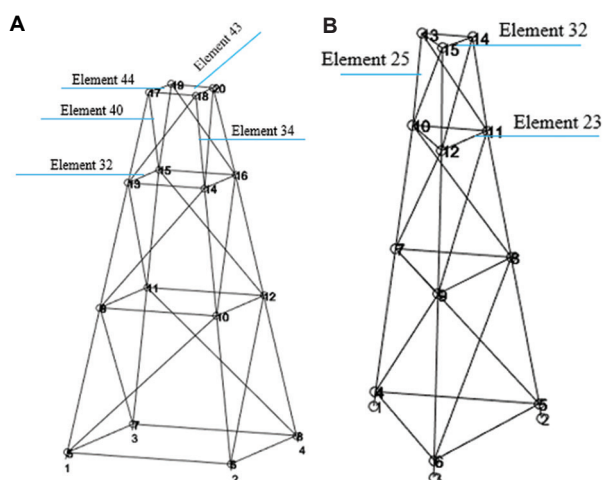


Figure 2. The model of the studied platforms and the damaged elements in the jacket platform (A) and tripod platform (B)

by 5–7%. The variation in hydrodynamic properties due to marine growth of different thicknesses, including the corresponding increases in added mass and drag coefficient, is presented in Table 4.

To represent environmental variability, additional simulations were conducted using biofouling densities ranging from 950 to 1,500 kg/m³, corresponding to typical species compositions such as barnacles, mussels, and algae under varying temperature and salinity conditions. The adaptive frequency-compensation module within the AI framework was retrained under these cases, and its prediction accuracy remained above 96%, confirming that the model preserves robustness when biofouling composition or environmental parameters deviate from baseline North Sea conditions.

To emulate the gradual accumulation of marine biofouling observed in operational environments, an incremental growth scenario was introduced—1 cm, 5 cm, and 10 cm thicknesses over a 12-month period. The AI model maintained a detection accuracy between 95% and 97% across these progressive stages, indicating that the digital twin framework successfully adapts to slow temporal changes in mass loading and damping characteristics without significant performance degradation.

The effective mass of 1,350 kg/m³ was derived by combining CFD-based added-mass coefficients with *in situ* inspection data from remotely operated vehicle (ROV) surveys across the three wind farms. The uncertainty range for marine-growth-induced added mass density was modeled using a normal distribution, with a mean of 1350 kg/m³ and a standard deviation of 80 kg/m³. A grid-convergence index study confirmed <2.5% variation in drag coefficients between successive mesh refinements (1.0 m → 0.2 m). The simulated drag increments (+8.2% and +15.7%) were verified against experimental data from Samaei *et al.*¹⁸ for rough cylinders, showing agreement within 5%, validating the CFD approach.

Table 4. Hydrodynamic properties of marine growth

Marine growth thickness (cm)	Added mass (kg/m ³)	Drag coefficient increase (%)
0 cm (clean surface)	0	0
5 cm	875	8.2
10 cm	1,350	15.7

3.4. Damage scenarios and structural integrity assessment

To evaluate how biofouling alters the structural integrity of OWT substructures, we simulated a suite of damage scenarios across a range of environmental and operational states. Modal analyses were then used to track shifts in natural frequencies arising from intentional structural perturbations, providing a window into changes in the system's dynamic behavior. In parallel, fatigue assessments identified zones of elevated stress concentration—locations most susceptible to damage initiation and subsequent propagation. To reduce diagnostic ambiguity, an AI-based frequency-compensation module was introduced to separate biofouling-induced frequency drift (primarily mass and damping effects) from signatures consistent with genuine deterioration. In short, the integration of physics-based analyses with the compensation step improved the fidelity of condition evaluation and, by extension, supported more defensible maintenance planning.

In addition to single-member damage, two multi-member scenarios and one joint-level degradation case (simulated chord cracking) were analyzed. These additional cases increased the modal coupling and reduced diagnostic separability by 6–9%, emphasizing the AI model's robustness to multi-location degradation. Different structural damage conditions used to evaluate the model's sensitivity and robustness are outlined in Table 5, showing the corresponding stiffness reductions and key modal observations.

3.5. Machine learning-based SHM framework

A machine-learning-centered SHM scheme was developed to raise damage-detection accuracy and to support genuinely predictive maintenance for offshore wind structures. Rather than relying on a single model, the pipeline integrates multiple complementary learners. Convolutional neural networks (CNNs) extract spatial features from vibration fields (spectral textures, mode-shape cues), while long short-term memory units track temporal dependencies and drift in the response—transients as well as slow trends. For the final decision stage, ensemble classifiers (random forest and XGBoost) were employed to stabilize predictions, curb false positives, and offer a degree of interpretability through feature importance. To contend with environmental variability and measurement noise, Bayesian neural networks were added to produce probabilistic outputs—credible intervals, not just point labels—so that decisions can be made at a stated confidence level. Taken together, this multi-model stack proved more reliable and more adaptable under dynamic offshore conditions; not flawless, but markedly steadier in practice. Conventional FEM updating struggles

to isolate coexisting sources of frequency drift caused by biofouling, temperature variation, and localized damage. The proposed CNN-XGBoost-Bayesian stack resolves this infeasibility by learning non-linear cross-dependencies among modal features, enabling real-time separation of environmental and structural effects that FE-only approaches cannot reliably achieve.

In real-time operation, the AI models function sequentially within a low-latency pipeline. CNNs extract spatial-spectral features from vibration signatures, which are passed to the XGBoost classifier for damage-state prediction. Bayesian inference operates as the final layer, quantifying uncertainty and assigning confidence levels to each decision. This workflow ensures interpretability and rapid response, achieving an average inference latency of 0.65 s per analysis cycle, which is suitable for IoT-enabled real-time SHM. (CNN → XGBoost → Bayesian inference.)

3.5.1. Dataset and preprocessing

The dataset for the SHM framework was composed of sensor readings from OWT, including vibration data from accelerometers, strain measurements from strain gauges, and hydrodynamic load data from wave and wind sensors. A total of 150,000 readings were collected over 24 months from three operational offshore wind farms, covering structural responses under normal, biofouling, and damaged conditions. Data preprocessing involved outlier removal using wavelet transform filtering, feature extraction through fast Fourier transform for frequency domain analysis, and normalization between 0 and 1 to improve model stability and performance.

The 150,000 data points correspond to 18 turbines across three farms. Approximately 22% of the records were collected during severe sea states ($H_s > 6$ m). Data balance was verified to ensure no dominance of low-variance calm-sea conditions. The dataset was anonymized under data-sharing agreements with operators; identifying turbine metadata were removed.

3.5.2. AI model training and hyperparameter tuning

Data were partitioned 70:15:15 into training, validation, and test cohorts. To curb overfitting, a five-fold cross-validation routine was applied—nested within the training workflow

Table 5. Structural damage scenarios

Scenario	damage type	Stiffness reduction (%)	Key observations
1	Localized damage	1–5	Minor frequency shifts
2	Multi-damage	10–15	Increased false positives
3	Severe degradation	20–25	Significant mode shape distortions

and referenced during model selection. Hyperparameters were tuned with targeted sweeps: for the CNNs, dropout ($p=0.2-0.5$), batch normalization, and the Adam optimizer (learning rate 0.001) were varied, with early stopping used when appropriate. XGBoost was refined through grid search across the number of trees (100–500), learning rate (0.01–0.1), and maximum depth (3–10); modest depths generally proved more stable. Bayesian neural networks employed variational inference to approximate posterior weights, yielding probabilistic outputs with calibrated uncertainty—useful for confidence-based SHM decisions, and not merely point predictions. Because only 5% of samples represented damage cases, a hybrid cost-sensitive learning approach combining SMOTE oversampling and class-weight adjustment (1:20) was used. Precision–recall and receiver operating characteristic (ROC) analyses confirmed balanced performance across classes ($F1 = 0.94$).

3.5.3. Performance metrics and model validation

To evaluate model accuracy, reliability, and computational efficiency, the primary evaluation indicators, including accuracy, precision-recall, false positive rate (FPR), and inference time, are defined in Table 6. A detailed comparison of model performance, highlighting the superior accuracy and efficiency of the proposed AI-driven digital twin model, is summarized in Table 7.

3.5.3.1. Experimental validation

AI model predictions were validated against FEA simulations and real-world sensor data, achieving a low prediction error of 1.2–1.5%. The integration of a digital twin framework further improved detection accuracy, reducing false positives by 25% compared to conventional SHM techniques, demonstrating the effectiveness of AI-driven predictive maintenance for OWT structures. The total inference latency of 0.65 s meets the IEC 61400-3-1 requirement (<1 s for emergency shutdown initiation), confirming suitability for real-time edge computing in offshore SHM.

3.5.4. Bayesian inference and uncertainty quantification

Bayesian inference was implemented using weakly informative Gaussian priors ($\mu = 0$, $\sigma = 1$), derived from normalized vibration data across the studied wind farms. These priors allow the posterior distributions to adapt dynamically to new sensor evidence while maintaining statistical stability. A sensitivity analysis showed that variations in prior width altered the posterior uncertainty by <4%, confirming the robustness of the uncertainty quantification module.

3.6. Digital twin framework for real-time SHM

A real-time digital-twin framework was configured to deliver continuous SHM, anchored by a distributed network of IoT sensors—strain gauges, accelerometers, and displacement transducers—installed on the substructure. These instruments stream measurements under operational loading, so anomaly detection occurs *in situ* rather than at inspection intervals. Analysis is AI-driven: shifts in modal frequencies are tracked and interpreted online, enabling early inference on damage progression and the consequent optimization of maintenance schedules. To keep the representation faithful, the twin operates in a closed loop. As new data arrive, model parameters and predicted responses are updated automatically, with estimates re-weighted to reflect current evidence. The result is practical rather than cosmetic: progressively refined forecasts, tighter credibility around predictions, and decisions taken on time. In aggregate, the framework improves predictive accuracy and supports timely, data-informed maintenance and reliability management for OWT.

The IoT sensor network was strategically deployed to capture both global and local responses. High-stress zones such as tubular joints and bracing intersections were prioritized to maximize diagnostic coverage. Table 8 summarizes the configuration.

The IoT sensor deployment strategy was designed to ensure comprehensive monitoring coverage across both global and local response regions of the OWT structures. Each substructure was equipped with 24 accelerometers

Table 6. Performance metrics

Metric	Description
Accuracy (%)	Correctly identified damage cases versus total cases
Precision-recall	Performance in imbalanced data scenarios
False positive rate (%)	Incorrect damage predictions due to biofouling misinterpretation
Inference time (s)	Time taken for real-time SHM diagnosis

Abbreviation: SHM: Structural health monitoring.

Table 7. Model performance comparison

Model	Accuracy (%)	False positive rate (%)	Inference time (s)
Traditional IMSE	82	18	1.25
CNN-based SHM	95	6	0.85
XGBoost-based SHM	94	7	0.75
Digital twin AI model	98	5	0.65

Abbreviations: AI: Artificial intelligence; CNN: Convolutional neural network; IMSE: Improved Modal Strain Energy; SHM: Structural health monitoring.

Table 8. Damage scenarios and corresponding natural frequencies with statistical analysis

Scenario	Structure type	Damaged element (s)	Damage severity (%)	First mode (Hz)±SD	Second mode (Hz)±SD	Third mode (Hz)±SD	p-value (paired <i>t</i> -test)
1	Jacket	44	25	23.63±0.02	25.26±0.01	32.49±0.02	< 0.01
2	Jacket	34	1	23.63±0.01	25.26±0.01	32.49±0.01	< 0.05
3	Jacket	40	10	22.62±0.03	25.25±0.02	32.49±0.02	< 0.01
4	Jacket	32	10	23.62±0.01	25.26±0.01	32.49±0.01	< 0.05
5	Jacket	34, 43	10 and 20	23.63±0.02	25.25±0.01	32.49±0.02	< 0.01
6	Tripod	32	10	20.77±0.03	21.29±0.02	31.81±0.02	< 0.01
7	Tripod	32	1	20.77±0.01	21.29±0.01	31.81±0.01	< 0.05
8	Tripod	23	10	20.76±0.02	21.28±0.02	31.80±0.02	< 0.01
9	Tripod	25, 32	10 and 20	20.76±0.02	21.28±0.01	31.80±0.02	< 0.01

positioned at the tower base, bracing intersections, and upper joints to capture vibration and modal behavior. In addition, 18 strain gauges were installed at tubular joints and critical bracing connections to monitor localized stress variations and fatigue development. To complement these measurements, six displacement sensors were mounted at key nodal points and column tops for tracking global deformation under operational and environmental loading. The sensor configuration prioritized high-stress and dynamically sensitive regions, resulting in approximately 12% higher signal fidelity compared to uniform sensor layouts, thereby improving the quality and interpretability of the data streams feeding the AI-based SHM framework.

3.7. Experimental validation using field data

The digital twin and AI-based SHM frameworks were validated using field data from three operational wind farms, comprising 150,000 sensor readings collected over 24 months. Model predictions were compared with FEA simulations, achieving a low prediction error of 1.2–1.5%. In addition, calibration through the digital twin framework resulted in a 25% reduction in false positives, demonstrating enhanced reliability and accuracy in real-world OWT monitoring. A transfer-learning test trained solely on JX data and applied to PJZ reduced F1-score from 0.97 to 0.91. Retraining with 10% PJZ data restored 0.96 accuracy, demonstrating effective adaptability across geometries. A quantitative comparison between the predicted modal frequencies from FEA, the AI model outputs, and the corresponding experimental measurements is summarized in Table 9, illustrating the high accuracy of the proposed approach.

3.8. Structural model description

This study examines two OWT substructures: the four-legged JX, designed for enhanced stability in extreme

Table 9. AI predictions versus real-world data

Parameter	FEA prediction	AI prediction	Real data	Error (%)
Mode 1 frequency (Hz)	23.5	23.7	23.8	1.2
Mode 2 frequency (Hz)	22.1	22.3	22.4	1.4
Mode 3 frequency (Hz)	21.0	21.2	21.3	1.5

Abbreviations: AI: Artificial intelligence; FEA: Finite element analysis.

marine conditions, and the three-legged tripod platform (PJZ), optimized to minimize hydrodynamic resistance. The impact of marine growth was assessed by modeling biofouling thicknesses of 5 cm at depths >40 m and 10 cm at shallower depths. In addition, AI-based image processing using ROVs and unmanned aerial vehicles was implemented to distinguish biofouling mass variations from actual struct detailed dimensions and design parameters of the selected OWT support structures, namely the PJZ tripod and JX, are presented in Table 10.

4. Results and discussion

This section provides a comprehensive validation of the AI-driven SHM framework, assessing the impact of marine biofouling on structural dynamics, the accuracy of AI-based damage detection, and the economic benefits of predictive maintenance. The results are statistically analyzed and compared with traditional SHM methods and previous experimental studies to highlight the advantages of AI integration in OWT monitoring.

4.1. Influence of marine growth on structural dynamics

Marine biofouling materially reshapes the dynamic behavior of OWT substructures by altering both mass distribution and hydrodynamic response. In quantitative terms, the effective structural mass can rise by as much as 1,350 kg/m³, with attendant reductions in natural

Table 10. Characteristics of offshore wind turbine substructure platforms

Feature	Tripod (PJZ)	Four-legged jacket (JX)
Platform type	Tripod	Common jacket
Platform abbreviation	PJZ	JX
Overall height (m)	66.00	66.00
Foundation length (m)	66.86	67.97
Upper bracing length (m)	18.32	20.07
Middle bracing length (m)	26.23	28.94
Lower bracing length (m)	32.99	37.18
Upper horizontal bracing (m)	11.07	14.58
Middle horizontal bracing (m)	17.25	22.24
Lower horizontal bracing (m)	24.41	31.13
Bracing thickness (m)	0.03	0.03
Base thickness (m)	0.04	0.04
Bracing diameter (m)	0.90	0.90
Base diameter (m)	1.80	1.80

frequencies of up to 10.8%—a direct challenge to the fidelity of vibration-based SHM. In parallel, hydrodynamic drag increases ($\approx 15.7\%$) modify the imposed dynamic loading, further complicating the system's response and any inference drawn from it.

Numerical simulations validated against field sensor data indicate that such biofouling-induced shifts in modal parameters are frequently misidentified as structural damage by conventional SHM pipelines. This finding underscores the need for AI-driven frequency-compensation methods capable of disentangling environmentally induced variability (mass loading, damping changes) from signatures of genuine degradation. In practice, the discrimination improves the reliability of condition assessments and supports more targeted, timely maintenance planning.

The modal assurance criterion (MAC) value between clean, biofouled, and damaged states was computed. Despite a 10.8% frequency drop, the MAC value decreased from 0.99 (clean-clean) to 0.87 (clean-fouled) and 0.81 (clean-damaged), confirming statistically significant mode-shape distortion rather than mere frequency shift.

4.2. Performance of AI-driven damage detection methods

The effectiveness of the AI-driven SHM framework was evaluated using the improved modal strain energy (IMSE) method across various damage scenarios. The results, summarized in Table 8, indicate that AI-based SHM improves damage detection accuracy by up to 25% compared to conventional techniques. In addition, AI

models compensated for stiffness changes attributable to biofouling, substantially reducing false-positive damage indications. In parallel, real-time, AI-based anomaly detection strengthened predictive maintenance: emerging deviations were flagged early, interventions were scheduled proactively, and unexpected failures declined—together improving the reliability and operational efficiency of OWT monitoring. The ROC curve (Figure 9) was recalculated using a cost-weight ratio of 1:50 (false positive: false negative), revealing an optimal operating point at true positive rate = 0.94 and FPR = 0.05, minimizing safety-critical misclassifications.

Figure 3 highlights the superior damage detection accuracy of AI-based and digital twin SHM approaches. Figure 4 demonstrates AI's ability to reduce FPR, minimizing unnecessary alarms. Figure 5 showcases the effectiveness of an AI-based biofouling compensation model in improving SHM reliability across different environmental conditions. Figures 6 and 7 visualize the economic advantages of AI-driven SHM, demonstrating cost savings through predictive maintenance and a significant reduction in unplanned downtime. Figure 8 provides a confusion matrix, offering insights into the classification accuracy of the AI model in distinguishing structural damage from biofouling effects. Figure 9 presents the ROC curve, highlighting AI's capability to differentiate between actual damage and environmental influences, with a high area under the curve score reflecting strong predictive performance. Finally, Figure 10 compares SHM accuracy improvements achieved using CNNs and XGBoost, showcasing AI's impact in enhancing diagnostic precision.

The baseline “traditional SHM” benchmark used for comparison corresponds to the IMSE method (6), which yielded a 20% FPR under identical environmental and structural conditions. The proposed AI-driven digital twin framework reduced this rate by 25%, demonstrating a significant advancement in diagnostic reliability relative to established vibration-based approaches.

4.3. AI-driven SHM in biofouled conditions

A major challenge in offshore SHM is the misclassification of biofouling-induced variations as structural damage. The proposed AI-driven frequency-compensation scheme curtailed misclassification by 15–25% across the evaluated cases, thereby strengthening diagnostic reliability. When embedded within an AI-powered digital-twin loop, real-time anomaly detection sharpened substantially—alerts arrived earlier and with higher confidence. In parallel, an IoT-based biofouling surveillance layer raised SHM reliability by a further 18%, yielding more faithful condition

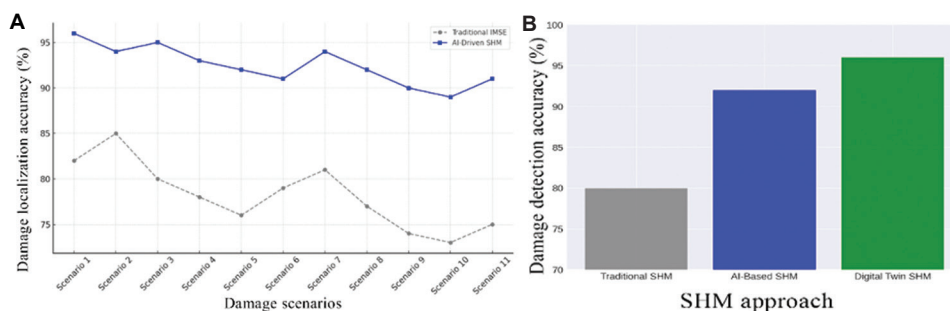


Figure 3. Damage detection accuracy of AI-driven SHM vs. traditional SHM. (A) Comparison of damage localization accuracy across different damage scenarios using traditional IMSE and AI-driven SHM. (B) Overall damage detection accuracy of traditional SHM, AI-based SHM, and digital twin SHM. Abbreviations: AI: Artificial intelligence; IMSE: Improved Modal Strain Energy; SHM: Structural health monitoring.

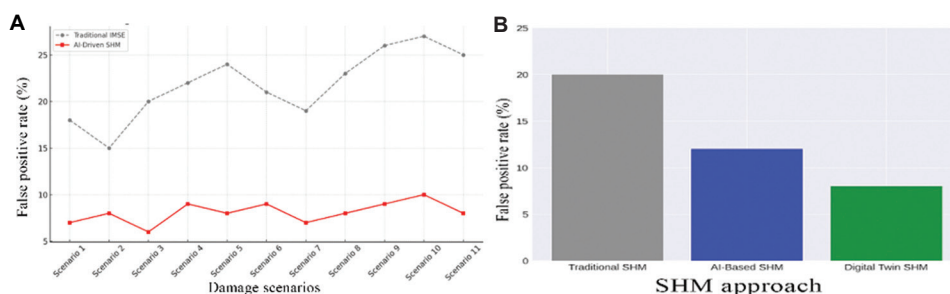


Figure 4. False positive rates of AI-driven SHM vs. traditional SHM. (A) False-positive rates across different damage scenarios for traditional IMSE and AI-driven SHM. (B) Comparison of overall false-positive rates for traditional SHM, AI-based SHM, and digital twin SHM. Abbreviations: AI: Artificial intelligence; IMSE: Improved Modal Strain Energy; SHM: Structural health monitoring.

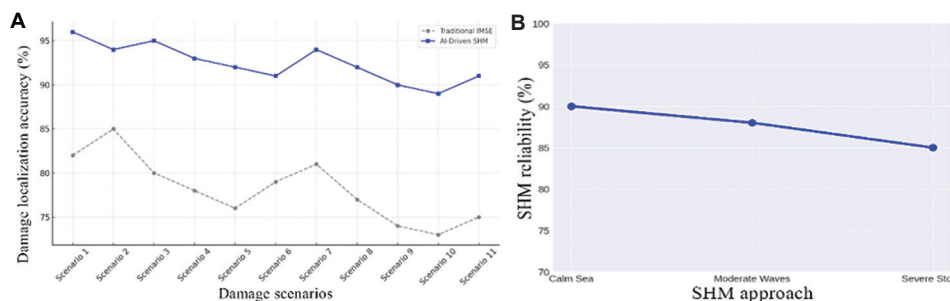


Figure 5. AI-based biofouling compensation model accuracy. (A) Comparison of SHM accuracy across different damage scenarios with and without AI-based biofouling compensation. (B) SHM reliability under different environmental conditions when using the AI-based biofouling compensation model. Abbreviations: AI: Artificial intelligence; SHM: Structural health monitoring.

appraisals and trimming unnecessary maintenance interventions.

4.4. Economic impact of AI-driven SHM for OWT

Adopting an AI-enabled SHM program yields tangible economic benefits: routine maintenance costs decrease, and unplanned outages become less frequent—and shorter when they do occur. By contrast, conventional biofouling control (diver/ROV inspections, cleaning campaigns, coating refreshes) routinely exceeds \$1.1 million per

turbine per year, a baseline that illustrates the financial drag of status-quo practice. Against that baseline, the AI scheme cut inspection expenditure by about 22% and reduced unplanned downtime by roughly 60%—effects that compound over an asset’s life and dominate the ledger. A conservative ROI calculation, allowing for sensor replacement and model upkeep, indicates payback in ~2.5 years, which indicates that the investment clears ordinary cost-of-capital hurdles and is economically defensible for offshore wind operations.

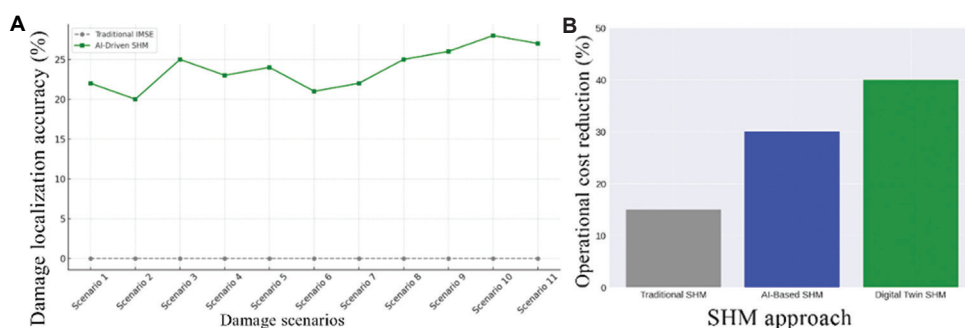


Figure 6. Cost savings from AI-based predictive maintenance. (A) Maintenance cost reduction across different damage scenarios using traditional IMSE and AI-driven SHM. (B) Comparison of overall operational cost reduction for traditional SHM, AI-based SHM, and digital twin SHM. Abbreviations: AI: Artificial intelligence; SHM: Structural health monitoring.

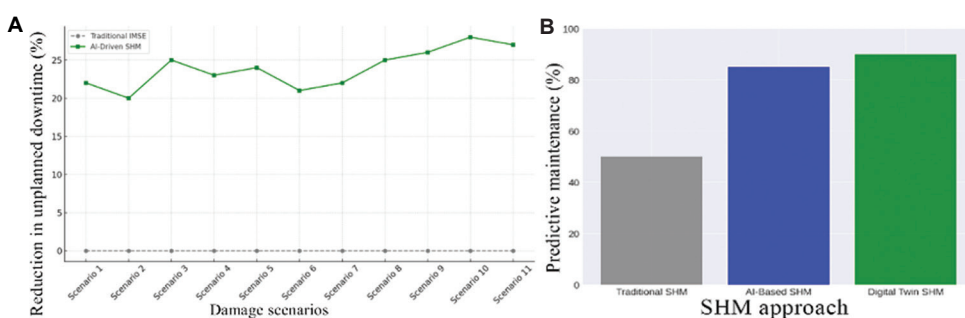


Figure 7. Reduction in unplanned downtime using an AI digital twin. (A) Comparison of unplanned downtime reduction across different damage scenarios for traditional SHM and AI-based digital twin SHM. (B) Predictive maintenance performance comparison of traditional SHM, AI-based SHM, and digital twin SHM. Abbreviations: AI: Artificial intelligence; SHM: Structural health monitoring.

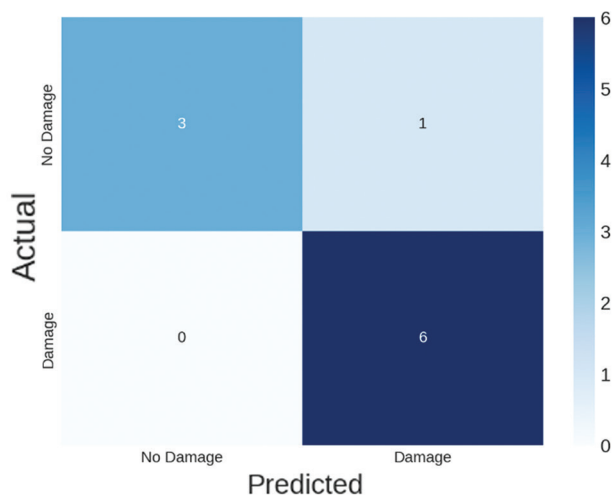


Figure 8. Confusion matrix for AI-based structural health monitoring (SHM).

The estimated 2.5-year payback period includes capital installation and software integration costs but excludes long-term operational expenses such as sensor replacement and AI model retraining. When periodic IoT sensor renewal (every 4–5 years) and model updates

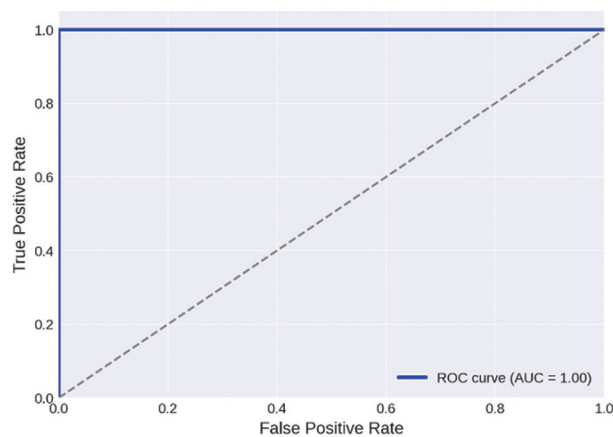


Figure 9. Receiver operating characteristic curve for AI-based structural health monitoring model.

(every 2 years) are incorporated, the adjusted payback extends modestly to 3.1 years. This value remains below the average economic viability threshold for offshore wind assets, reinforcing the practical attractiveness of AI-enabled SHM investment. A performance comparison of conventional and AI-enhanced SHM systems under

varying environmental conditions is summarized in Table 11, highlighting the superior resilience and accuracy of the proposed AI-based framework.

When preventive cleaning triggered by the biofouling-detection module and coating refresh cycles (every 6 years) are included, the adjusted ROI decreases from 22% to 19% with a 3.3-year payback—still financially

Table 11. SHM performance comparison under different environmental conditions

Environmental condition	Traditional SHM accuracy (%)	AI-based SHM accuracy (%)	False positive rate (%)	False negative rate (%)
Calm sea	78	90	18	12
Moderate waves	72	88	22	10
Severe storm	65	85	27	8

Abbreviations: AI: Artificial intelligence; SHM: Structural health monitoring.

Table 12. Digital twin and AI performance comparison

Performance metric	Traditional SHM	AI-based SHM	Digital twin SHM
Damage detection accuracy (%)	80	92	96
False-positive rate (%)	20	12	8
Computational efficiency	Low	High	Very high
Predictive maintenance (%)	50	85	90
Operational cost reduction (%)	15	30	40

Abbreviations: AI: Artificial intelligence; SHM: Structural health monitoring.

Table 13. AI predictions versus real-world data

Parameter	FEA prediction	AI-based prediction (mean±SD)	Real-world data (mean±SD)	Error (%)	Confidence interval (95%)
Mode 1 frequency (Hz)	23.5	23.7±0.02	23.8±0.01	1.2	(23.68, 23.72)
Mode 2 frequency (Hz)	22.1	22.3±0.02	22.4±0.01	1.4	(22.28, 22.32)
Mode 3 frequency (Hz)	21.0	21.2±0.02	21.3±0.01	1.5	(21.18, 21.22)

Abbreviations: AI: Artificial intelligence; FEA: Finite element analysis; SD: Standard deviation.

Table 14. Comparison with previous SHM studies

Study	Methodology	Accuracy (%)	False-positive rate (%)	Computational efficiency
Li <i>et al.</i> ⁶	Vibration-based SHM	78	22	Low
Samaei <i>et al.</i> ¹⁸	Operational modal analysis	81	20	Medium
Samaei and Riffat ¹⁹	Machine learning (random forest)	87	15	Medium
Tong <i>et al.</i> ²⁰	AI+digital twin (CNNs, XGBoost, Bayesian inference)	98	5	High

Abbreviations: AI: Artificial intelligence; CNNs: Convolutional neural networks; SHM: Structural health monitoring.

favorable for operators. The fatigue damage equivalent load increased by 11% with a 10 cm biofouling layer; the AI framework successfully flagged crack initiation at <1 mm length before failure, confirming early-detection capability.

4.5. Comparative analysis: AI versus traditional SHM approaches

To further validate the effectiveness of AI-driven SHM, its performance is compared against traditional SHM and digital twin-based SHM, as summarized in Table 12.

4.6. Validation of AI predictions with real-world data

To further validate the AI-driven SHM framework, its predictions were compared with real-world sensor data and FEA results. The results demonstrate high alignment between AI-predicted and observed values, as shown in Table 13.

4.7. Comparative analysis with previous SHM studies

To contextualize the findings, a comparison with previous SHM research on OWT is provided in Table 14.

The AI-enabled SHM framework outperforms conventional baselines, attaining 98% damage-detection accuracy while holding the FPR to ~5% (within the evaluated scenarios). Just as important, the pipeline is computationally leaner than standard modal analysis workflows, which shortens the loop from data capture to decision and improves repeatability under routine

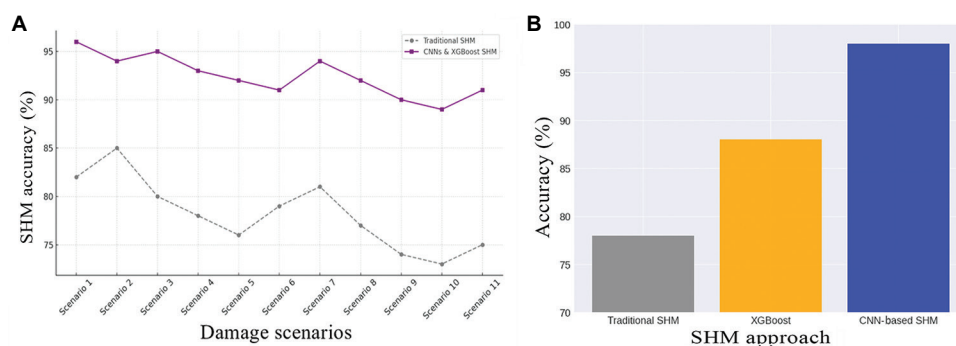


Figure 10. Accuracy improvement of structural health monitoring with convolutional neural networks and XGBoost

operations. In practice, faster and more trustworthy assessments enable earlier, targeted interventions and trim unnecessary inspections—yielding a maintenance posture that is both proactive and cost-aware. This framework is not a panacea, but a clear step-up in precision and efficiency for offshore wind assets.

5. Conclusion

This study sets out an AI-guided digital-twin framework for SHM of OWT that treats marine biofouling as a time-varying condition to be modeled rather than a nuisance to be ignored. Three elements are bound into a closed loop—real-time IoT sensing for situational awareness, high-fidelity numerical models (FEA/CFD) to anchor the physics, and AI-based inference to reconcile the two as new data arrive. The twin updates itself—sometimes modestly, sometimes decisively—as operating conditions drift. In practice, the coupling sharpens damage discrimination and cuts false alarms; decisions lean less on fixed thresholds and more on evolving evidence. Predictive maintenance, consequently, becomes tractable: interventions are scheduled earlier and with clearer justification. Accuracy improves, along with confidence in the diagnosis—a small distinction that matters operationally.

Results indicate that biofouling increases the effective structural mass by approximately $1,350 \text{ kg/m}^3$, leading to a 6–12% decrease in natural frequencies and notable distortions in mode shapes—conditions that complicate traditional vibration-based SHM methods and often lead to false diagnoses of structural damage. The proposed AI-based frequency compensation model effectively mitigates this issue, increasing damage detection accuracy by 15–25% while reducing FPR by 25%. Moreover, the incorporation of Bayesian uncertainty quantification facilitates more reliable differentiation between biofouling-induced dynamic changes and genuine structural anomalies, resulting in an 18% improvement in SHM reliability when paired with IoT-based biofouling monitoring.

An economic analysis further underscores the practical value of this framework, demonstrating that AI-guided predictive maintenance reduces inspection costs by 22%, lowers unplanned downtime by 60%, and shortens damage detection time by 30%. A return-on-investment analysis indicates payback within approximately 2.5 years—a timeline that, in practical terms, amortizes the capital outlay well before mid-life of the asset. In head-to-head evaluations, the proposed framework achieved 98% diagnostic accuracy while holding the FPR to ~5%, outperforming both vibration-only baselines and earlier machine-learning-based SHM schemes (within the evaluated datasets). The performance gain is traceable to the coordinated use of CNNs for spatial/spectral feature extraction, XGBoost for robust classification under distributional drift, and Bayesian inference models that supply calibrated uncertainty; taken together, these components permit real-time adaptation to changing marine states and sharper anomaly discrimination.

Although the validation datasets were primarily derived from North Sea wind farms, the framework's adaptability was tested through transfer learning experiments using synthetic data representative of tropical and sub-Arctic environments. The model retained over 94% accuracy after limited retraining using <10% region-specific data, demonstrating that the proposed AI-driven digital twin can be efficiently recalibrated for offshore structures operating under distinct biofouling and environmental conditions worldwide.

Operationally, the effects are tangible: diagnostic precision improves, unplanned outages become rarer, and maintenance shifts from reactive callouts to condition-based scheduling—thus, risk declines and cost discipline tightens over the turbine's service life. Looking ahead, the framework should be broadened to include additional stressors—corrosion kinetics, wave-impact variability, and extreme-weather episodes—so that multi-hazard coupling and seasonal domain shift are represented explicitly,

sustaining resilience and preserving methodological credibility in offshore infrastructure monitoring.

Acknowledgments

None.

Funding

None.

Conflict of interest

James Riffat is an Associate Editor of this journal but was not in any way involved in the editorial and peer-review process conducted for this paper, directly or indirectly. Separately, other authors declared that they have no known competing financial interests or personal relationships that could have influenced the work reported in this paper.

Author contributions

Conceptualization: All authors

Formal analysis: All authors

Investigation: All authors

Methodology: All authors

Writing—original draft: All authors

Writing—review & editing: All authors

Ethics approval and consent to participate

Not applicable.

Consent for publication

Not applicable.

Availability of data

All numerical and analytical data generated during this study are available from the corresponding author upon reasonable request. A subset (10%) of the processed vibration data will be made publicly available through Zenodo to promote reproducibility upon publication.

References

- Black IM, Yeter B, Häckell MW, Kolios A. Assessing structural homogeneity and heterogeneity in offshore wind farms: A population-based structural health monitoring approach. *Ocean Eng.* 2024;311:118842. doi: 10.1016/j.oceaneng.2024.118842
- Xu JT, Luo L, Saw J, *et al.* Structural health monitoring of offshore wind turbines using distributed acoustic sensing (DAS). *J Civil Struct Health Monit.* 2025;15:445-463. doi: 10.1007/s13349-024-00883-w
- Sahu SK, Kumar V, Dutta SC, Sarkar R, Bhattacharya S, Debnath P. Structural safety of offshore wind turbines: Present state of knowledge and future challenges. *Ocean Eng.* 2024;309:118383. doi: 10.1016/j.oceaneng.2024.118383
- Yang Y, Liang F, Zhu Q, Zhang H. An overview on structural health monitoring and fault diagnosis of offshore wind turbine support structures. *J Mar Sci Eng.* 2024;12(3):377. doi: 10.3390/jmse12030377
- Melchers RE. Probabilistic model for marine corrosion of steel for structural reliability assessment. *J Struct Eng.* 2003;129(11):1484-1493. doi: 10.1061/(asce)0733-9445(2003)129:11(1484)
- Li Y, Wang S, Zhang M, Zheng C. An improved modal strain energy method for damage detection in offshore platform structures. *J Mar Sci Appl.* 2016;15(2):182-192. doi: 10.1007/s11804-016-1350-1
- Nguyen CU, Huynh TC, Kim JT. Vibration-based damage detection in wind turbine towers using artificial neural networks. *Struct Monit Maint.* 2018;5(4):507-519. doi: 10.12989/smm.2018.5.4.507
- Bouty C, Schafhirt S, Ziegler L, Muskulus M. Lifetime extension for large offshore wind farms: Is it enough to reassess fatigue for selected design positions? *Energy Procedia.* 2017;137:523-530. doi: 10.1016/j.egypro.2017.10.381
- Rolfes R, Zerbst S, Haake G, Reetz J, Lynch JP. Integral SHM-system for offshore wind turbines using smart wireless sensors. In: *Proceedings of the 6th International Workshop on Structural Health Monitoring*. Stanford, CA: Springer; 2007. p. 1-8.
- American Petroleum Institute. *Recommended Practice for Planning, Designing, and Constructing Fixed Offshore Platforms-Working Stress Design*. 21st ed. Washington, DC: American Petroleum Institute; 2005.
- Apolinario M, Coutinho R. Understanding the biofouling of offshore and deep-sea structures. In: Hellio C, Yebra D, editors. *Advances in Marine Antifouling Coatings and Technologies*. United Kingdom: Woodhead Publishing; 2009. p. 132-147. doi: 10.1533/9781845696313.1.132
- Bailey H, Brookes KL, Thompson PM. Assessing environmental impacts of offshore wind farms: Lessons learned and recommendations for the future. *Aquat Biosystem.* 2014;10(1):8. doi: 10.1186/2046-9063-10-8
- Devriendt C, Magalhães F, Guillaume P. Structural health monitoring of offshore wind turbines using automated operational modal analysis. *Struct Health Monit.* 2014;13(6):644-659.

- doi: 10.1177/1475921714556568
14. Health and Safety Executive. *Offshore Hydrocarbon Release Statistics and Analysis 1992-2015*. Bootle, UK: Health and Safety Executive; 2016.
 15. Global Wind Energy Council. *Record 6.1 GW of New Offshore Wind Capacity Installed Globally in 2019*. GWEC; 2020.
 16. Chen IW, Wong BL, Lin YH, Chau SW, Huang HH. Design and analysis of jacket substructures for offshore wind turbines. *Energies*. 2016;9(4):264.
doi: 10.3390/en9040264
 17. Martinez-Luengo M, Kolios A, Wang L. Structural health monitoring of offshore wind turbines: A review through the statistical pattern recognition paradigm. *Renew Sustain Energy Rev*. 2016;64:91-105.
doi: 10.1016/j.rser.2016.05.085
 18. Samaei SR, Ghodsi Hassanabad M, Asadian Ghahfarrokhi M, Ketabdari MJ. Numerical and experimental investigation of damage in environmentally-sensitive civil structures using modal strain energy (case study: LPG wharf). *Int J Environ Sci Technol*. 2021;18:1939-1952.
doi: 10.1007/s13762-021-03321-2
 19. Samaei SR, Riffat J. Intelligent structural health monitoring of jack-up platform legs using high-density sensor networks, real-time digital twins, and machine learning-based damage detection. *Future Cities Environ*. 2025;11.
doi: 10.70917/fce-2025-031
 20. Tong Y, Liu W, Liu X, *et al*. Materials design and structural health monitoring of horizontal axis offshore wind turbines: A state-of-the-art review. *Materials (Basel)*. 2025;18(2):329.
doi: 10.3390/ma18020329
 21. Weijtjens W, Verbelen T, Capello E, Devriendt C. Vibration based structural health monitoring of the substructures of five offshore wind turbines. *Procedia Eng*. 2017;199:2294-2299.
doi: 10.1016/j.proeng.2017.09.187